Meteorol. Atmos. Phys. 41, 127–145 (1989)

Meteorology and Atmospheric Physics

551.515.11

Institute of Earth Sciences, Free University of Amsterdam, Amsterdam, The Netherlands

On the Deepening and Filling of Balanced Cyclones by Diabatic Heating

A. van Delden*

With 18 Figures

Received November 11, 1988
Revised March 14, 1989

Summary

The results of computations of the radial circulation and associated surface pressure tendencies, needed to retain gradient wind balance in a model of an axisymmetric cyclone, due to the action of diabatic heating and boundary layer pumping, are presented. These computations show that diabatic heating will not induce further deepening (i.e. intensification) of the cyclone when this cyclone is weak and has a cold core. On the other hand, a relatively intense warm-core balanced cyclone will deepen appreciably, depending on the degree of baroclinicity and on where exactly the heat sources are located.

These results underline the fact that Conditional Instability of the Second Kind (CISK) must be interpreted as a finite-amplitude instability. CISK cannot explain the genesis of a cyclone, such as a polar low or hurricane.

1. Introduction

This paper is about "ideal" cyclones and the effect diabatic heating has on their *growth and decay*. An example of such an "ideal" cyclone is shown in Fig. 1. The main characteristics of this Mediterranean winter cyclone are the high degree of axisymmetry, the eye and the intense convection around the eye. Evidently, these hurricane-like cyclones are not confined only to the tropics or to the summer or early fall. Another characteristic of such a cyclone, which is not immediately evident on the satellite photograph, but has been observed in tropical cyclones, is the fact that gradient wind balance is usually very well satisfied, especially in mature (tropical) cyclones (see e.g. Willoughby, 1979; Sheets, 1982). These characteristics also apply, more or less, to polar lows, "bombs" and other Mediterranean convective vortices (see e.g. Scorer, 1986; Rasmussen and Lystad, 1987; Sanders and Gyakum, 1980; Billing et al., 1983; Rasmussen and Zick, 1987).

About 25 years ago Charney and Eliassen (1964), Ooyama (1964) and Ogura (1964) proposed a theory for the growth of a tropical hurricane depression. Much later this theory was also used by Rasmussen (1979) to explain the growth of polar lows. They showed that, if frictional convergence in the center of a vortex could force cumulus convection and latent heat release, this would disturb gradient wind balance in such a way that the vortex was bound to grow, in spite of the counter-effect of spin down due to Ekman layer pumping. This mechanism is now called conditional instability of the second kind (CISK). The theory of CISK has actually never been generally accepted as a theory for the growth of tropical cyclones (see e.g. Riehl, 1981; Emanuel, 1986), and has led to much debate and confusion among those

* Present address: Institute for meteorology and oceanography, University of Utrecht, Princetonplein 5, NL-3584 CC Utrecht, The Netherlands.

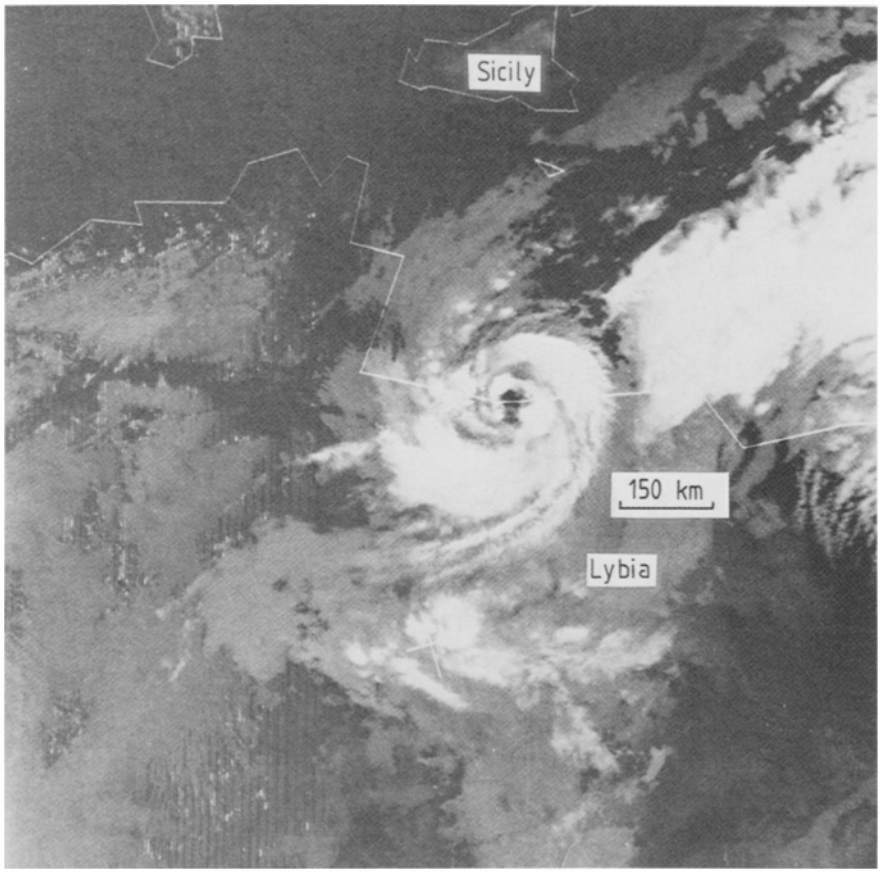

Fig. 1. Satellite-photograph (NOOA-6, infra-red) of a hurricane-like vortex making landfall at the Lybian coast on 15 december, 1985, 5: 35 UT

who do accept the basic philosophy (for a review see e.g. Ooyama, 1982).

Probably, the confusion has one of its roots in the fact that CISK, as presented by Charney and Eliassen (1964), is a linear instability, i.e., given a suitable environment, a (gradient wind-) balanced infinitesimal symmetric disturbance will amplify spontaneously. However, as Charney and Eliassen recognized, CISK is not a theory for the genesis or formation of a hurricane depression in the same way as static thermal instability is a theory for the genesis of convection currents. In their introduction, Charney and Eliassen (1964) admit that there must be a pre-existing balanced depression of at least small amplitude before CISK can start accounting for further intensification. But, in order to apply perturbation analysis, they are forced to assume that the depression has infinitesimal amplitude. Therefore their linear theory should not be taken too literally. It should be viewed as indicating the importance of processes in a small-amplitude system that could also be important in a finite-amplitude system.

More recently Schubert and Hack (1982), Shapiro and Willoughby (1982) and Hack and Schubert (1986) have shown that intense vortices in gradient wind balance react much more strongly to a specified heat source than weak balanced vortices. This could imply that CISK would become much more effective in a finite amplitude system than in an infinitesimal system.

In view of the confusion about the exact nature and applicability of CISK, and also of the studies performed by Schubert and Hack (1982, 1986), and Shapiro and Willoughby (1982), it appears worthwhile to extend the linear analysis of Charney and Eliassen (1964) and Ooyama (1964, 1969) to the finite-amplitude case, without considering the problem as an initial-value problem as is done in numerical simulations of balanced cyclones (e.g. Ooyama, 1969; Sundquist, 1970). The results of such an analysis, are described in this paper. This analysis is in fact very similar to those performed by Shapiro and Willoughby (1982) and Schubert and Hack (1982), except that boundary layer pumping is now included. Also, diabatic heating

is assumed proportional to boundary layer convergence, as in the theory of CISK, whereas in the former studies the diabatic heating-rate *and* -distribution was specified exactly.

In the present analysis the disturbances will possess more realistic tangential velocity profiles than the sine- or bessel-functions used in linear analysis. The "growth" of the depression will not be expressed in terms of the growth-rate of the perturbation (having dimension of $[\text{time}]^{-1}$), as in linear stability analysis, but in terms of the deepening-rate or surface-pressure decrease-rate (in millibar per hour), which appears more natural to this author.

The computations described in this paper will show that the central surface pressure decrease-rate depends strongly on cyclone-intensity and cyclone-baroclinicity. Cyclone-intensity is measured in terms of the maximum tangential wind-speed or the minimum surface pressure (Holland and Merrill, 1984). Cyclone-baroclinicity is measured in terms of the difference in the tangential wind-speeds between the inflow- and the outflow-layers.

The computations described in this paper show that the central surface pressure in relatively weak cyclones (maximum tangential velocity in the order of 10 m/s or less) is hardly affected by diabatic heating. On the other hand, relatively *intense warm core* cyclones may experience significant deepening (> 1 mb/hr) through diabatic heating. This is not always the case, however. In very intense and/or cold-core vortices the central surface pressure tendency may even become positive. This rather surprising result will be shown to be related to the decrease of the *local* Rossby radius of internal deformation in the core of the cyclone to values smaller than the radius of the eye. It is well known that diabatic heating cannot very effectively disturb gradient wind balance at distances much larger than the Rossby radius of deformation (see e.g. Gill, 1982). Therefore, since the bulk of the diabatic heating takes place in the eye-wall, this heating is not able to induce large negative surface pressure-tendencies in the center of the cyclone when the local Rossby radius in the heating region is much smaller than the radius of the eye.

It will be shown, furthermore, that the tendency of intense cyclones to fill depends also on whether the cyclone has a warm or a cold core. Because of the decrease of the tangential wind-speed with height, which makes the inertial resistance to the upper level outflow relatively weak, a warm core cyclone is more likely to deepen by diabatic heating, than a cold-core cyclone.

In this study we will assume that *the cyclone has to satisfy gradient wind balance at all times.* This assumption filters out gravity-inertia waves. Latent heat sources will continually disturb this balance. In order to maintain gradient wind balance, mass must be redistributed radially under the constraint of angular momentum conservation (if the disturbance is axisymmetric). The question why the flow- and mass-fields re-adjust to gradient wind balance when the mass-field is disturbed is not easily answered. According to the study by Schubert et al. (1980), the balance-assumption is valid best when the time scale of the process (for instance latent heat release), which is disturbing the balance of forces, is relatively long. Short period disturbances (much shorter than the time scale associated with inertial oscillations around the balanced state) will excite large-amplitude gravity-inertia waves and thus large departures from the balanced state. If the process which is disturbing gradient wind balance is related directly to the balanced flow, which is indeed the case in CISK (through Ekman-layer pumping), then obviously this process will possess the same time-scale as the balanced flow. Therefore, in the light of the study of Schubert et al. (1980), it appears reasonable to assume that, if the heating is forced by Ekman layer pumping, the flow is able to adjust continuously to gradient wind balance, without losing too much energy to gravity-inertia waves. Therefore, it is reasonable to investigate a problem in which gravity-inertia waves are ignored.

2. Gradient Wind Adjustment

CISK is in fact equivalent to continuous, perfect gradient wind adjustment of a vortex to self-induced disturbances of this state of balance. In this section it will be shown semiqualitatively why perfect and continuous gradient wind adjustment to disturbances in the mass-field may lead to a surface pressure decrease in the center of the cyclone and, thus, to further intensification of the cyclone. It is hoped that this will lay the basis to understand the results described subsequently.

Let us, to simplify the argumentation in this section, divide the free troposphere into two layers: the lower troposphere (layer 1) and the upper

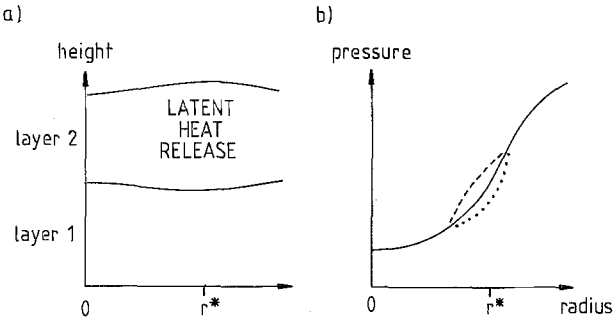

Fig. 2. a) Schematic two-layer representation of the troposphere. b) Hypothetical pressure-distribution in a balanced vortex. The dashed line indicates how the pressure-ditribution is altered in the upper layer after latent heat is released in an area centered at $r = r^*$. The dotted line indicates how the pressure distribution is altered in the lower layer due to outflow (from $r = r^*$) in the upper layer

troposphere (layer 2) (see Fig. 2a). Suppose that the air in these two layers is rotating with the *same* tangential speed, v, about an axis $r = 0$, where r is the radial coordinate. Suppose also that the resulting centrifugal and coriolis forces are in balance with a pressure force, i.e.

$$\frac{1}{\rho}\frac{\partial p}{\partial r} = \frac{v^2}{r} + fv, \tag{2.1}$$

where p is the pressure, ρ the density and f the corolis parameter. Suppose now that latent heat is released at $r = r^*$ in layer 2. A reason for this location of the heating rather than at $r = 0$ will be given at the end of section 3. Due to expansion of air, isobaric surfaces are elevated. The horizontal pressure gradient is altered in such a way that it increases for $r < r^*$ and decreases for $r > r^*$. To restore gradient wind balance, mass must be redistributed radially, *subject to the constraint of conservation of angular momentum.*

The angular momentum per unit mass, M, is defined as

$$M = vr + \frac{1}{2}fr^2, \tag{2.2}$$

which implies that,

$$v = \frac{M}{r} - \frac{1}{2}fr. \tag{2.3}$$

This, in turn, implies that the coriolis force per unit mass (F_{cor}) plus the centrifugal force per unit mass (F_{cen}) acting on the radially moving air must

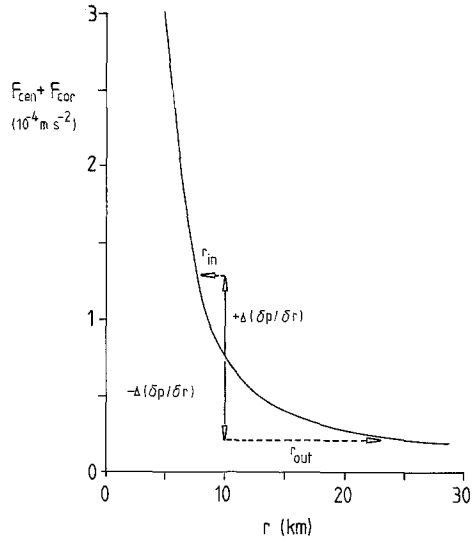

Fig. 3. The radial dependence of the centrifugal force (F_{cen}) plus the coriolis force (F_{cor}) under the contraint that the angular momentum (M) (2.2 with $f = 10^{-4}$) is constant, for $M = 0.5 \cdot 10^4 m^2 s^{-1}$. If the pressure-gradient force is altered by, say $\Delta(\partial p/\partial r)$, air must flow radially outwards or inwards, depending on the sign of $\Delta(\partial p/\partial r)$, to restore gradient wind balance

obey the following relation:

$$F_{cen} + F_{cor} = \left(\frac{v^2}{r} + fv\right) = \frac{M^2}{r^3} - \frac{1}{4}f^2 r \tag{2.4}$$

The right hand side of (2.4) is plotted in Fig. 3 as a function of r for a particular value of M. *A fluid parcel with fixed mass moving radially and conserving angular momentum, M, will experience a net outward force given by the function plotted in Fig. 3.* Evidently, ($F_{cen} + F_{cor}$) increases more than linearly with decreasing r.

If the pressure-gradient force in the upper layer is decreased (for $r > r^*$) by say $\Delta(\partial p/\partial r)$ due to latent heat release (see Fig. 2b), air must flow outwards over a distance r_{out} to restore gradient wind balance. Of course, this radial motion will automatically be attended with further changes in the pressure distribution, implying that the air may not have to flow exactly over a distance r_{out}. But let us, for simplicity, temporarily ignore this feedback effect.

The pressure-change in each layer is proportional to the total divergence above. The divergence is given by $(\partial u/\partial r + u/r)$, where u is the radial velocity. Therefore, the outflow in the upper layer will lead to a pressure-decrease in the lower layer. The pressure-gradient in the lower layer will

thus increase for $r > r^*$ (see Fig. 2b). Air must then flow inwards over a distance r_{in} (see Fig. 3) to restore gradient wind balance. If the disturbance in the pressure gradient in the lower layer (due to the outflow in the upper layer) is approximately equal in absolute value to the initial disturbance in the pressure-gradient in the upper layer (due to latent heat release), which seems to be a reasonable first-order accurate assumption, then $r_{out} > r_{in}$, i.e. the outflow is greater than the inflow, implying that the surface-pressure will decrease.

Note that the same argument applied to $r < r^*$ yields a reverse circulation, i.e. inflow in the upper layer and outflow in the lower layer (eye-formation).

Although this semi-qualitative analysis ignores the variations in the depth of the inflow and outflow layers as well as all the important feedback processes that take place during gradient wind adjustment, it does illustrate some essential features of this process. According to the above simplified analysis, *exact* gradient wind adjustment in an axisymmetric vortex, is very probably attended with a *surface pressure-decrease. This is essentially due to the fact that the radially flowing air must both conserve angular momentum and readjust to gradient wind balance.* Whether this surface pressure-decrease exceeds, in absolute value, the surface pressure-*increase* resulting from Ekman boundary layer pumping (one of the most important processes contributing to the filling and decay of the cyclone) is a question which has occupied many researchers in the past decades and which will be the main subject of this paper. Due to the slightly different approach to the problem we will in fact discover some new phenomena.

3. The Model Atmosphere

The model atmosphere is now assumed to consist of four "shallow water" layers of constant density (see Fig. 4). Layer zero (the boundary layer) exerts a stress on the earth, while the three layers above represent the "free" atmosphere. The density of the boundary layer, ρ_0, is equal to the density of the layer above, while the density of layers 2 and 3 is a factor ε and a smaller respectively, i.e. $\rho_0 = \rho_1 = \rho_2/\varepsilon = \rho_3/a\,(0 < \varepsilon < 1,\ a < \varepsilon)$. The parameter, $\sigma = 1 - \varepsilon$ is called the static stability. This model is therefore identical to Ooyama's

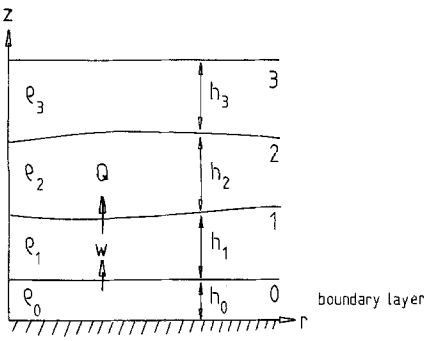

Fig. 4. Structure of the four-layer version of Ooyama's (1969) model

(1969) model, except that an additional layer (3) has been added in the same way in Smith's (1981) model of cyclostrophic adjustment. By varying the density, a, we can investigate the importance of the so-called "external mode", associated with the interface between layers 2 and 3. The upper free surface is assumed to be fixed so that the pressure gradient in the uppermost layer is equal to zero. The notation used in this section is identical to Ooyama's (1969) notation.

The thickness of layers 1, 2 and 3, h_1, h_2 and h_3 may vary, while the thickness of the boundary layer h_0, is constant. Convergence or divergence in the boundary layer leads to a vertical mass flux at the top of the boundary layer.

The pressure p is only dependent on r, z and t. The ground pressure is given by,

$$p_0 = g\rho\,(h_0 + h_1 + \varepsilon h_2 + a h_3)\,. \tag{3.1}$$

Instead of p, it is more convenient to use the geopotential, φ, defined in each layer as,

$$\varphi_j = (p_j - \bar{p}_j)/\rho_j\,,$$

where $\bar{p}_j$ is a standard reference pressure in layer j, corresponding to a height $\bar{h}_j$. In each layer the geopotential is defined as,

$$\varphi_0 = \varphi_1\,, \tag{3.2a}$$

$$\varphi_1 = g\,(h_1 + \varepsilon h_2 + a h_3 - (\bar{h}_1 + \varepsilon \bar{h}_2 + a \bar{h}_3))\,, \tag{3.2b}$$

$$\varphi_2 = g\,(h_1 + h_2 + \frac{a}{\varepsilon} h_3 - (\bar{h}_1 + \bar{h}_2 + \frac{a}{\varepsilon} \bar{h}_3))\,, \tag{3.2c}$$

$$\varphi_3 = g\,(h_1 + h_2 + h_3 - (\bar{h}_1 + \bar{h}_2 + \bar{h}_3))\,. \tag{3.2d}$$

We will assume that $\bar{h}_j = \bar{h}$ for $j = 1, 2$ and 3. We will also assume that the tangential (primary) flow above the boundary layer is in gradient-wind balance with the pressure field. This implies that,

$$f v_j^2 + v_j^2/r = \partial \varphi_j / \partial r \, (j = 1, 2, 3). \tag{3.3}$$

The radial motion is expressed in terms of a flux ψ_j, defined by,

$$\psi_j = \frac{-\rho_j}{\rho_0} h_j u_j r, \tag{3.4}$$

where u_j is the radial velocity in layer j. Conservation of mass for each of the main layers is expressed as,

$$\frac{\partial h_1}{\partial t} = \frac{\partial \psi_1}{r \partial r} - Q + w, \tag{3.5a}$$

$$\varepsilon \frac{\partial h_2}{\partial t} = \frac{\partial \psi_2}{r \partial r} + Q, \tag{3.5b}$$

$$a \frac{\partial h_3}{\partial t} = \frac{\partial \psi_3}{r \partial r}, \tag{3.5c}$$

where w is the vertical velocity at the top of the boundary layer. Diabatic processes (e.g. latent heat release due to cumulus convection) are represented as a vertical mass-flux, $\rho_1 Q$, from layer 1 to layer 2. Q has the dimension of velocity. Due to the heat source, the upper layer grows at the cost of the lower layer. Thus, *diabatic heating causes an upward bulging of surfaces of equal pressure. This effect is responsible for cyclone intensification. It is worthwhile noting here that sensible heat fluxes from the ocean also have this effect on the surfaces of equal pressure.* The diabatic term is set proportional to the boundary layer convergence as

$$Q = \eta w^+, \tag{3.6}$$

where $w^+ = w$ when $w > 0$ and zero otherwise and η is a nondimensional parameter which depends, among other, on the equivalent potential temperature of the boundary layer air and the equivalent potential temperature-stratification (Ooyama, 1969). It is treated as a free parameter here.

Conservation of angular momentum in each main layer combined with conservation of mass (3.5a, b, c) yields three prognostic equations for the tangential flow velocities, v_1, v_2, v_3 analogous to Ooyama's (1969) equations (3.15):

$$\frac{\partial v_1 r}{\partial t} = h_1^{-1} (f + \zeta_1) \psi_1 + \frac{w^+}{h_1} (v_0 - v_1) r + \frac{1}{h_1} \frac{\partial \Lambda_1}{r \partial r}, \tag{3.7a}$$

$$\frac{\partial v_2 r}{\partial t} = (\varepsilon h_2)^{-1} (f + \zeta_2) \psi_2 + \frac{Q}{\varepsilon h_2} (v_1 - v_2) r + \frac{1}{h_2} \frac{\partial \Lambda_2}{r \partial r}, \tag{3.7b}$$

$$\frac{\partial v_3 r}{\partial t} = (a h_3)^{-1} f \psi_3 + \frac{1}{h_3} \frac{\partial \Lambda_3}{r \partial r}, \tag{3.7c}$$

where ζ_j is the vertical component of the relative vorticity, i.e.

$$\zeta_j = \frac{\partial v_j}{\partial r} + \frac{v_j}{r}. \tag{3.8}$$

Λ_j are the radial fluxes of angular momentum due to lateral eddy transport per unit radian of air in layer j:

$$\Lambda_j = \lambda_j h_j r^3 \frac{\rho_j}{\rho_0} \frac{\partial}{\partial r} \frac{v_j}{r}, \tag{3.9}$$

where λ_j are the kinematic coefficients of eddy-viscosity.

Equations (3.7a, b, c), together with (3.3) (gradient wind balance), (3.2a, b, c, d) (hydrostatic balance) and (3.5a, b, c) (conservation of mass), are only compatible when the radial (secondary) flow (ψ_j) obeys the following three equations,

$$r \frac{\partial}{\partial r} \frac{1}{r} \frac{\partial}{\partial r} (\psi_1 + \psi_2 + \psi_3) - S_1 \psi_1 = B_1, \tag{3.10a}$$

$$r \frac{\partial}{\partial r} \frac{1}{r} \frac{\partial}{\partial r} \left(\psi_1 + \frac{1}{\varepsilon} (\psi_2 + \psi_3) \right) - \frac{1}{\varepsilon} S_2 \psi_2 = B_2, \tag{3.10b}$$

$$r \frac{\partial}{\partial r} \frac{1}{r} \frac{\partial}{\partial r} \left(\psi_1 + \frac{1}{\varepsilon} \psi_2 + \frac{1}{a} \psi_3 \right) - \frac{1}{a} S_3 \psi_3 = B_3, \tag{3.10c}$$

where for $j = 1, 2, 3$,

$$S_j = \left(f + \frac{2 v_j}{r} \right) \frac{f + \zeta_j}{g h_j}, \tag{3.11a}$$

$$B_j = \frac{1}{g} \left\{ \left(f + \frac{2 v_j}{r} \right) F_j - r \frac{\partial G_j}{\partial r} \right\}. \tag{3.11b}$$

S_j is a measure for the inertial stability in layer j and B_j is the forcing due to the redistribution of angular momentum F_j and mass G_j. G_j and F_j are defined as

$$G_1 = g w;$$
$$G_2 = G_3 = g(w + \varepsilon^{-1} \sigma Q), \tag{3.12a}$$

$$F_1 = \frac{1}{h_1 r} \frac{\partial A_1}{\partial r};$$
$$F_2 = \frac{1}{\varepsilon h_2} \left\{ Q(v_1 - v_2) r + \frac{\partial A_2}{r \partial r} \right\};$$
$$F_3 = \frac{1}{a h_3 r} \frac{\partial A_3}{\partial r}. \tag{3.12b}$$

The expression for F_1 implies that $v_0 = v_1$. This approximation will be discussed at the end of this section. In (3.12b) effects of diabatic cooling and (internal) friction between the two main layers, which were included in the model of Ooyama (1969), are neglected here. *The purpose is to calculate the solution of (3.10a, b, c) for a prescribed tangential flow.* If the absolute vorticity associated with this tangential flow is everywhere positive, then a solution exists (see Ooyama, 1969). When a solution has been obtained, the surface pressure-tendency as a function of r can be calculated with the help of

$$\frac{\partial p_0}{\partial t} = g \rho_0 \left(\frac{\partial (\psi_1 + \psi_2 + \psi_3)}{r \partial r} + w \right), \tag{3.13}$$

which has been derived from (3.1) and (3.5a, b, c). Clearly, the pressure-change is determined by the divergence in the upper three layers and the mass pumped into the lower layer (1) due to Ekman pumping. *The cyclonic depression will deepen and intensify if* $\partial p_0 / \partial t < 0$ *at* $r = 0$. If it is negative, we will refer to $|\partial p_0 / \partial t|$ $(r = 0)$ as the intensification- or deepening-rate of the cyclone. The method of solution of (3.10 a, b, c) and (3.13) is described in the appendix.

But, before these equations can be solved, w must be linked to the prescribed tangential flow above the boundary layer. Ooyama (1969) assumed that internal friction or eddy dissipation in the boundary layer could be ignored compared to surface friction (proportional to $C_D |v_0| v_0$, where C_D is the drag coefficient). The resulting boundary layer pumping formula is then very different to the form used in linear studies of CISK, in which the vertical velocity at the top of the boundary layer is proportional to the vorticity aloft. Ooyama's (1969) equation for the vertical velocity at the top of the boundary layer is,

$$w = \frac{C_D}{r} \frac{\partial}{\partial r} \left\{ \frac{|v_1| v_1 r}{\zeta_1 + f} \right\}. \tag{3.14}$$

We can deduce from this equation that $w = 0$ at the point where $v_1 = 0$, i.e. at $r = 0$, *implying that boundary layer convergence is zero in the center of the vortex and has a maximum somewhere at finite radius.* This agrees with the analysis of Eliassen (1971) and also with the conclusions of Yamasaki (1977).

To arrive at the above formula, Ooyama (1969) assumed that the boundary layer was in a steady state and that $v_0 = v_1$. Some justification for the assumption, $v_0 = v_1$ can be found in the paper by Schubert and DeMaria (1985b), who integrated Ooyama's model without the above assumptions and indeed find that $v_0 \approx v_1$ (see Fig. 2 in their paper). The assumption of a steady state implies that the boundary layer adjusts instantaneously to changes in the atmosphere above.

Linear Analysis

Ooyama (1969, section 8) performed a linear instability analysis of his three-layer model in which he examined the growth of small balanced perturbations superposed on a fluid system at rest. In this analysis he neglected the effects of curvature and assumed a linear dependence of the stress with the earth's surface on the boundary-layer wind velocity, which yields $w = (k_s/f) \zeta_1$, where k_s is a positive constant, defined in Ooyama (1969). He also assumed unconditional heating and took h_1 and h_2 constant $(= h)$. He substituted a solution of the form

$$\varphi_j = \Phi_j e^{\gamma t} \sin \left\{ \frac{\pi r}{2l} \right\}, \tag{4.1}$$

where Φ_j is a constant, γ the growth rate of the perturbation and l the quarter wavelength (the radius of maximum wind). It is straightforward to repeat this analysis (with $\lambda_j = 0$) for the present four-layer version of the model. The result is that

the growth rate is given by

$$\gamma = \frac{\left(1 - \frac{\frac{a}{\varepsilon} - 1}{\sigma \xi^2}\right) \frac{k_s}{h \xi^4} (\eta - 1 - \xi^2)}{\left(1 + \frac{1}{\xi^2}\right)^2 \left(1 - \frac{\frac{a}{\varepsilon} - 1}{\sigma \xi^2} + \frac{a}{\varepsilon \xi^2}\right) - \varepsilon \left(1 - \frac{\frac{a}{\varepsilon} - 1}{\sigma \xi^2}\right)}, \tag{4.2}$$

where the nondimensional scale parameter ξ is defined by

$$\xi^2 = \frac{2 l^2}{(\pi R)^2}, \tag{4.3}$$

and R is the Rossby radius of internal deformation defined in this model by

$$R = \left\{\frac{\sigma g h}{2}\right\}^{1/2} \frac{1}{f}. \tag{4.4}$$

The sign of γ is determined by the factor $(\eta - 1 - \xi^2)$. Instability (CISK) occurs when $\eta > 1 + \xi^2$, implying that the inhibiting effect of the earth's rotation (i.e. the inertial stability) on the radial circulation is most appreciable at scales larger than the Rossby radius. Therefore, the system will prefer to be smaller than the Rossby radius of deformation, such that $\xi^2 << 1$.

In view of the fact that CISK is most relevant to cyclones of finite amplitude, a sensible and interesting question is whether the same kind of criterion for growth of the cyclone continues to be valid when it possesses larger amplitudes. If this is so, not only the earth's rotation, but also the rotation of the flow itself will influence the radial circulation. Then, as was also pointed out by Schubert and Hack (1982) and Ooyama (1982), the coriolis parameter, f, in the definition of R will have to be replaced by $(f + \zeta)$. This yields a "local" Rossby radius:

$$R_{loc} = \left\{\frac{\sigma g h}{2}\right\}^{1/2} \frac{1}{f + \zeta}, \tag{4.5}$$

as opposed to the "planetary" Rossby radius defined in (4.4). The local Rossby radius decreases strongly with increasing vorticity (see also Fig. 16 of Shapiro and Willoughby 1982). As the cyclone intensifies, there will presumably come a point when the criterion for intensification is no longer satisfied, *even if* η *remains constant*. Therefore, given η, there will presumably be an upper limit to the intensity of a warm-core cyclone, if it intensifies through CISK.

In the remaining part of this paper we will find out that this is indeed the case, although the reasons for the existence of an upper limit to the intensity will turn ot to be a bit more subtle than implied by the above linear analysis. Instead of a disturbance of the type given by (4.1), we will assume more realistic tangential velocity profiles and calculate the radial circulation which is needed to retain gradient wind balance under the action of (latent) heat sources, forced by Ekman pumping, and Ekman pumping itself, which of course also acts to disturb gradient wind balance.

5. The Tangential Velocity Profiles

Two types of tangential velocity profiles were prescribed. The first one, which will be called the "O-profile", is the most simple. It is given by,

$$v_j = \frac{2 v^* r}{r^* \left(1 + \left\{\frac{r}{r^*}\right\}^2\right)} \quad (j = 1, 2), \tag{5.1}$$

where v^* is the maximum tangential wind velocity and r^* is the radius of maximum wind (RMW). The above wind profile can be regarded as an approximation to the so-called "rankine-vortex" wind profile in which there is solid rotation (constant vorticity) in the center of the cyclone ($r < r^*$) and no vorticity outside $r = r^*$. The "O-profile" allows for a relatively simple interpretation of the calculations. It is, however, not the most realistic profile. Therefore, for completeness, we will also investigate a class of profiles which, according to Holland (1980), are representative for hurricanes, but probably also for other axisymmetric vortices, such as some polar lows. This profile, which will be called the "H-profile", is given by,

$$v_j = \left\{\frac{A B (p_n - p_c) \exp\left\{\frac{-A}{r^B}\right\}}{\rho r^B} + \frac{r^2 f^2}{4}\right\}^{1/2} - \frac{rf}{2} \quad (j = 1, 2), \tag{5.2}$$

where A and B are scaling parameters, p_c is the

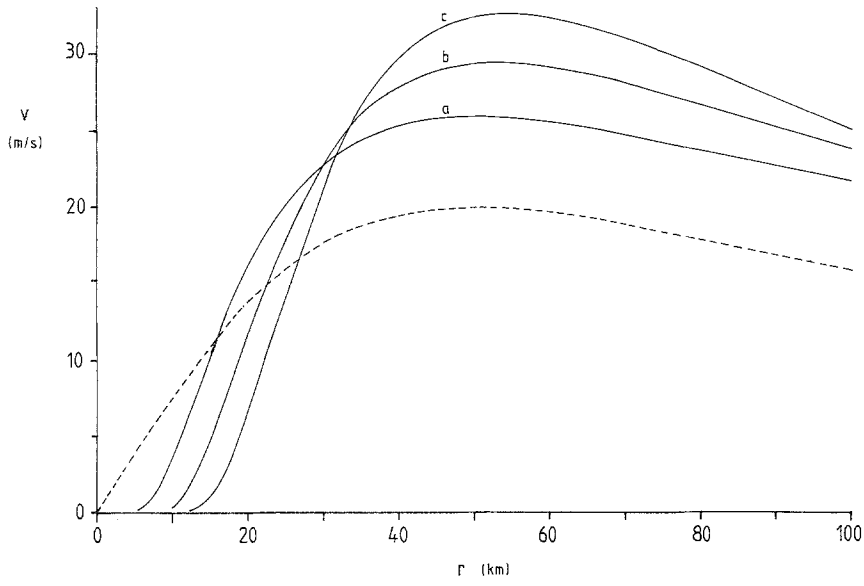

Fig. 5. Examples of the prescribed tangential velocity profiles. Dashed line: "O-profile" with $r^* = 50$ km and $v^* = 20$ m/s. Solid lines: H-profiles with (a) $B = 1.1$; (b) $B = 1.4$ and (c) $B = 1.7$, respectively ($p_n - p_c = 20$ mb, $r^* = 50$ km, $\rho = 1\,\mathrm{kg/m^3}$, $f = 10^{-4}\,s^{-1}$)

central ($r = 0$) surface pressure and p_n the ambient surface pressure (at infinite radius). Because the maximum wind does not enter into this equation, we will frequently take $(p_n - p_c)$ as a measure of the intensity of the cyclone, although, as we will see later the two are not perfectly correlated. The quantity $(p_n - p_c)$ can also be interpreted as the "depth" of the cyclone. If the coriolis force is small compared to the pressure-gradient and centrifugal forces, the RMW is given by (Holland, 1980):

$$r^* = A^{1/B}. \tag{5.3}$$

B determines the shape of the profile.

Holland (1980) compared several measured hurricane profiles with (5.2) and found values of B between 1.05 and 1.5. Examples of the velocity profiles investigated in this study are plotted in Fig. 5. In the case of the "H-profiles", the pressure-drop and the highest wind-speeds are concentrated more and more near the RMW as B increases. It can be seen that the maximum tangential wind-speed may increase when the profile changes shape, even though the minimum pressure remains constant.

6. The Radial Circulation and Associated Surface Pressure Changes

The pressure (or geopotential) profile associated with the prescribed tangential velocity profile is calculated on a grid by integrating (3.3) from $r = 0$ *outwards*. The corresponding layer thickness, h_j, is then obtained from (3.2). After the determination of w, S_j, B_j, G_j and F_j at each grid point for prescribed values of ε, a, η, λ, f and ρ, (3.10a, b, c) can be solved iteratively. Because it is desirable to have the best resolution near $r = 0$ (so that the central pressure decrease can be calculated accurately), the equations are solved on a grid which is stretched away from $r = 0$. The technical details of the solution-procedure are given in appendix A.

In this section we will discuss in some detail the solutions for a barotropic vortex with an "O-profile" (5.1), with $r^* = 50$ km, $\varepsilon = 0.9$, $a = 0.1$, $\rho = 1\,\mathrm{kg/m^3}$, $f = 10^4\,\mathrm{s}^{-1}$, $h_0 = 1\,000$ m, $\bar{h} = 5\,000$ m, $C_D = 0.0015$, $\lambda_j = 0$ (no lateral diffusion), $\eta = 2$ and $v^* = 27$ and 50 m/s, respectively.

This implies that the cyclone is at least 11 km deep. Polar lows usually do not extend to such great heights. The effect of the depth of the vortex on its intensification will be investigated in section 9.

The radial velocity profiles associated with these two tangential velocity profiles are shown in Fig. 6. It can be seen that the radial velocities are relatively very weak in the eye. Relating this to the argument in section 2, this is essentially due to the steepness of the curves, $(F_{cor} + F_{cen})$ (plotted in Fig. 3) in the core of the cyclone.

The surface pressure changes associated with these radial motions can be calculated from (3.13). The result is plotted in Fig. 7 for both the intense and the weaker vortex. Also shown are the profiles

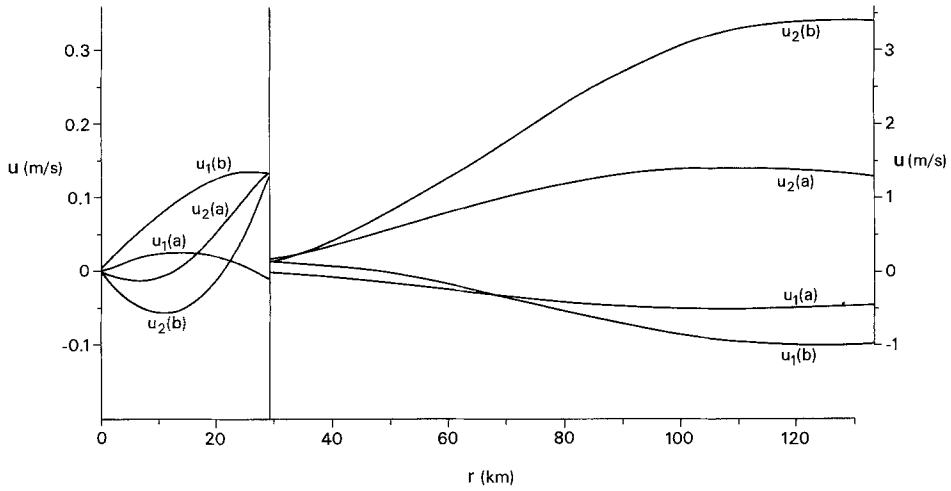

Fig. 6. Radial velocity profiles in a barotropic ($v_1 = v_2$) vortex possessing an "O"-tangential velocity profile (with $r^* = 50$ km) with $v^* = 27$ m/s (a) and $v^* = 50$ m/s (b), respectively. The vertical scale for $r < 28$ km is magnified 10 times compared to the vertical scale for $r > 28$ km. The parameters-values are: $\varepsilon = 0.9$, $\alpha = 0.1$, $\rho = 1\,\text{kg/m}^3$, $f = 10^{-4}\,s^{-1}$, $C_D = 0.0015$, $\lambda_j = 0$ ($j = 1$, 2, 3), $h_0 = 1\,000$ m, $\eta = 2$ and $\bar{h} = 5\,000$ m

of w. Evidently, the greatest forcing is located near the RMW. The surface pressure decrease rate is greatest just inside the RMW. Near the center of the cyclone p_0 decreases by about 0.32 mb/hr when $v^* = 27$ m/s and increases by about 0.53 mb/hr when $v^* = 50$ m/s, implying that the cyclone will not deepen further when $v^* = 50$ m/s. The surface pressure tendencies will lead to "flattening" of the surface pressure-profile in the center of the vortex (promoting a relatively calm eye) and an increase of the surface pressure-gradient just near the RMW. This process is displayed in Fig. 8 for the deepening cyclone ($v^* = 27$ m/s) and the filling cyclone ($v^* = 50$ m/s).

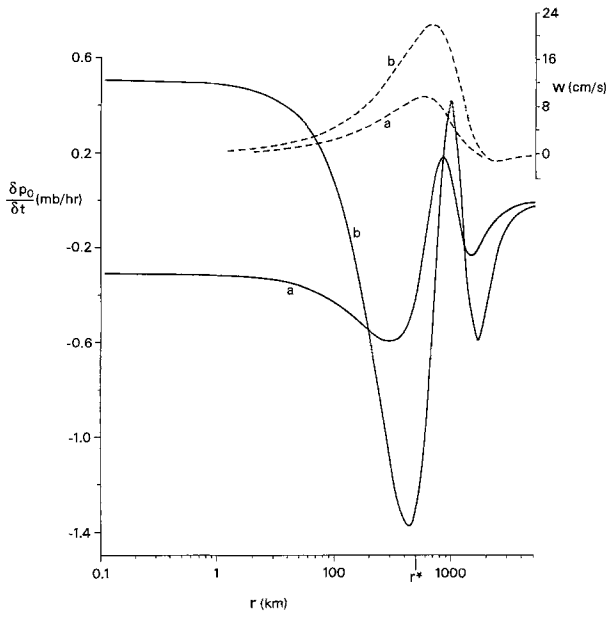

Fig. 7. The vertical velocity, w (dashed line), at the top of the boundary layer and the surface pressure-tendency (solid line) as a function of the radius in a barotropic vortex possessing an "O"-tangential velocity profile (see Fig. 5) with $r^* = 50$ km in two cases: (a) $v^* = 27$ m/s and (b) $v^* = 50$ m/s. The values of the other parameters are given in Fig. 6

In the case of the filling cyclone, the central vorticity is equal to 37.10^{-4} s^{-1}. This make the local Rossby radius, R_{loc}, equal to 13 km. The local Rossby radius at large radii, where $\zeta \approx 0$, (i.e. $R_{loc} = R$) is equal to 495 km. The radius of the eye (defined as the average radius (averaged over layers 1 and 2) at which the radial velocity changes sign) (see Fig. 6) in the filling cyclone is about 30 km. Thus, the eye circulation is much larger than the local Rossby radius. In the terms used by Frank (1983), one would say that the eye is "dynamically large". This is probably not very advantageous for the (central) deepening of the cyclone. The diabatic heating, which is concentrated at the outer edge of the eye (the eye-wall), is located at a dynamically large distance from the center of the cyclone. In the case of the deepening cyclone ($v^* = 27$ m/s), R_{loc} in the center of the cyclone and the mean radius of the eye are approximately equal to each other (21 km), which is, as we shall see later, the optimum configuration for cyclone intensification.

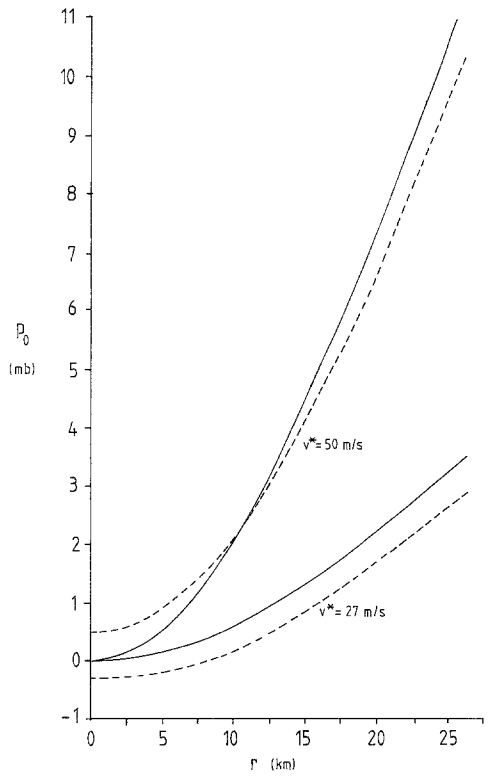

Fig. 8. Radial surface pressure profiles (solid lines) associated with the "O"-tangential velocity profile with $v^* = 27$ m/s (deepening cyclone) and $v^* = 50$ m/s (filling cyclone), respectively. Also shown are the radial surface pressure profiles (broken lines) one hour later, assuming the calculated (initial) pressure-tendencies (see Fig. 7) remain constant. The pressure p_0 is measured in mb relative to the initial pressure at $r = 0$. See Fig. 6 for the values of other parameters ($\nu_1 = \nu_2$)

At this point we may conclude that the reduction of η (the intensity of the diabatic heating) is not the only possible reason for the filling of cyclones. We will return to this remarkable fact in sections 8 and 9. But, before that we will shortly discuss the effect, on the central deepening rate, of lateral diffusion and changes in a as a function of the horizontal scale of the vortex.

7. The Central Surface Pressure-Tendency as a Function of Horizontal Scale or Radius of Maximum Wind

Figure 9 shows the central surface-tendency ($\partial p_0/\partial t$ ($r = 0$)), calculated according to the method described in appendix B, as a function of r^* (i. e. the RMW) for a vortex with a "H-profile" (5.2), with $p_n = 1010$ mb, $p_c = 990$ mb and $B = 1.4$, for three cases in which λ_j and a are varied. The values of the other parameters are identical to those used in the previous section. Without lateral diffusion, there is no so-called "small scale cut-off", i. e. the central deepening rate increase with decreasing scale of the vortex, at least until $r^* = 10$ km. Lateral diffusion has very little effect on the surface pressure tendency when the RMW is larger than 90 km. However, for small vortices ($r^* <$ km), lateral diffusion turns a deepening cyclone into a filling cyclone. For identical parameter-values, Ooyama (1969) finds, in his linear instability analysis, that the growth-rate (in s^{-1}) becomes negative when l (the quarter wavelength of the disturbance) (see section 4) becomes smaller than about 30 km. This quantitative agreement is encouraging. Apparently, the growth-rate of linear analysis and the central surface pressure tendency used in the present analysis, as measures of the intensification of the system, are comparable. However, the agreement is also a bit surprising, since the unrealistic (sine) tangential velocity profile assumed in the linear analysis differs greatly from the much more realistic "H-profile". Besides, the conditional nature of the heating, which is

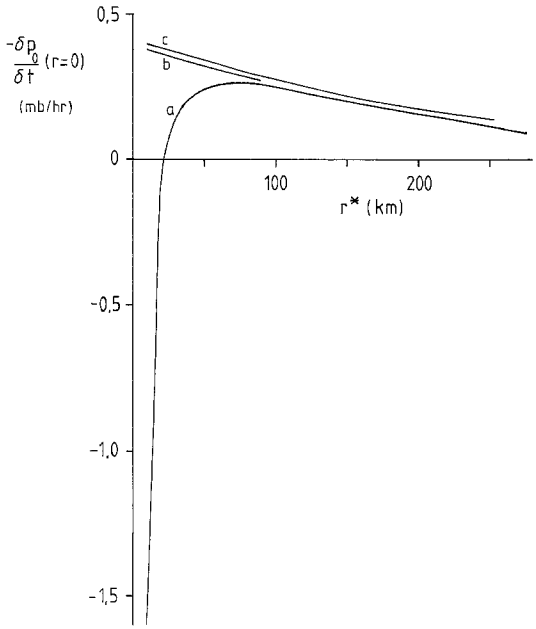

Fig. 9. The central surface pressure decrease-rate as a function of the horizontal scale or radius of maximum wind, r^*, in a barotropic vortex with an H-tangential velocity profile (see Fig. 5), with $p_n = 1010$ mb, $p_c = 990$ and $B = 1.4$ for three cases: a) $a = 0.1$, $\lambda_j = 1000\,m^2/s$; b) $a = 0.1$, $\lambda_j = 0$; c) $a = 0.5$, $\lambda_j = 0$. See Fig. 6 for the values of other parameters ($\nu_1 = \nu_2$)

known to have a great influence on the horizontal scale of motion in the case of moist convection (see e.g. van Delden, 1985), does not appear to have a great influence in this case. Also, boundary layer convergence in linear theory has its maximum in the center of the cyclone, which is not the case in the present nonlinear model, which assumes that boundary layer friction is dominated by surface friction (see Eliassen, 1971; Yamasaki, 1977; and 3.14).

In the next section it will become clear, from computations of the central surface pressure tendency as a function of vortex intensity, that there is in fact a very fundamental difference between the result of this analysis of the intensification and the result obtained from linear growth-rate analysis.

In the remaining part of this paper we will ignore lateral diffusion ($\lambda_j = 0$ for $j = 1, 2, 3$), since this effect makes the analysis of the problem more difficult and, also, it does not appear to have a great effect on the deepening-rate of cyclones with realistic horizontal dimensions. Moreover, the exact values of λ_j in the atmosphere are not known.

The curves (b) and (c) in Fig. 9 nearly coincide. It may thus be concluded that the external mode, associated with the interface between layers 2 and 3, is unimportant in determining surface pressure changes. In other words, *the deepening-rate is relatively insensitive to the value of α.*

8. The Central Surface Pressure Tendency as a Function of Cyclone-Intensity

Fig. 10 shows the central surface pressure tendency $\partial p_0/\partial t$ ($r = 0$) as a function of cyclone-intensity (v^*) for the "O-profile", for different values of η and r^*. Below a certain optimum value of v^*, the central surface deepening rate increases with increasing v^* for all cases, while it decreases abruptly and strongly for larger values of v^*. This implies that, as indicated by the results described in section 6, a cyclone cannot intensify indefinitely through CISK. The maximum intensity attainable through CISK, now measured in terms of the maximum tangential wind velocity, v^*_{max}, increases with η. This is shown in Fig. 11 for $r^* = 25$ km and $r^* = 100$ km. In both cases shown, v^*_{max} approaches zero as η decreases to one. This agrees with the linear stability criterion derived in section 4.

Vortices with $v^* < 5$ m/s (depth of about 2 mb) deepen at a rate less than 0.01 mb/hr. It would take the cyclone *at least* 200 hrs (8 days) to reach an intensity such that $v^* = 5$ m/s, provided $\eta < 2.5$. On the other hand, when $v^* \approx 25$ m/s, the central deepening rate has increased to values greater than 0.2 mb/hr (for $\eta \approx 2$). That is, the vortex-intensity has increased five-fold, while the central deepening rate has increased twenty-fold. Therefore, the deepening- or intensification-rate of the cyclone increases more than linearly with

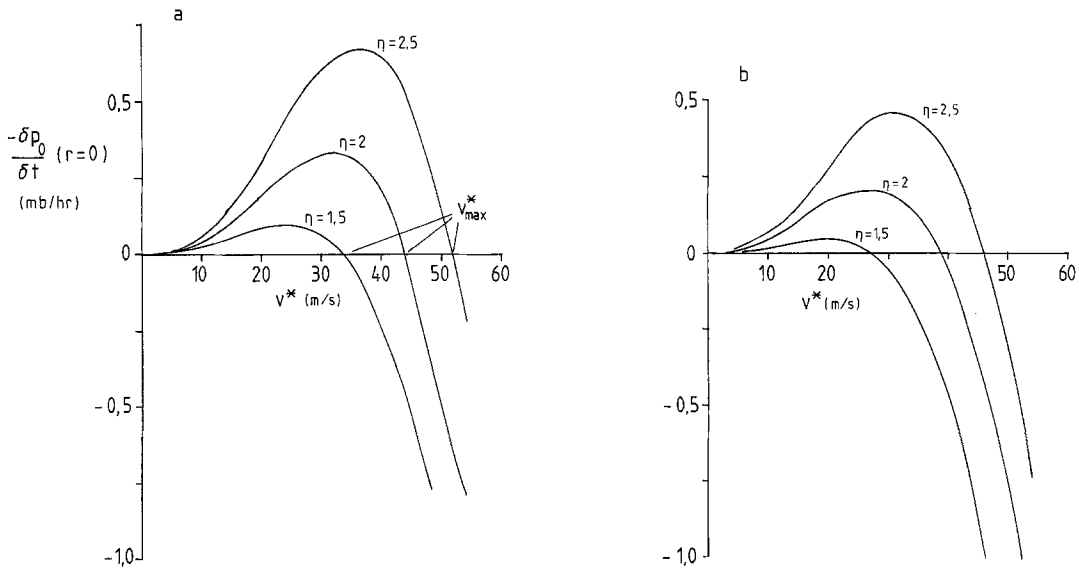

Fig. 10. The central surface pressure decrease-rate as a function of vortex-intensity, v^* ("O"-profile), for several values of η and a) $r^* = 25$ km; b) $r^* = 100$ km. See Fig. 6 for the values of other parameters ($\nu_1 = \nu_2$)

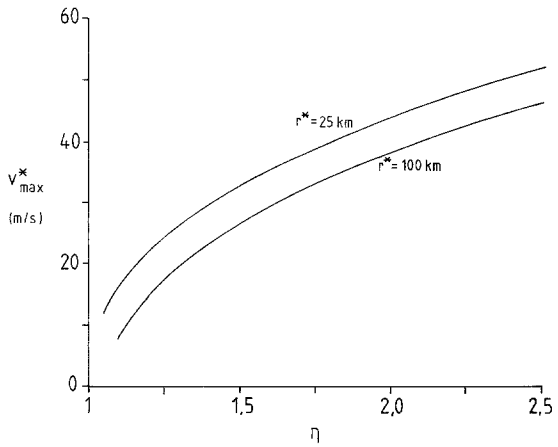

Fig. 11. Maximum attainable vortex-intensity, v^*_{max} (see Fig. 10 for the definition), as a function of η for vortices with an "O"-tangential velocity profile for $r^* = 25$ km and $r^* = 100$ km, respectively. See Fig. 6 for the values of other parameters ($\nu_1 = \nu_2$)

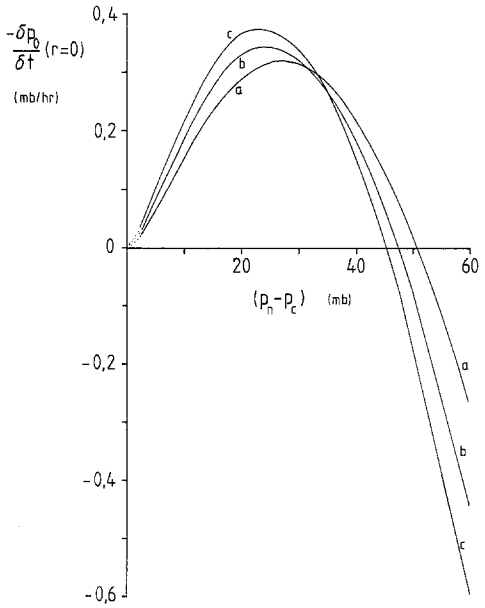

Fig. 12. The central surface pressure decrease-rate as a function of vortex-intensity, $(p_n - p_c)$ ("H-profile"), for several values of B (the shape of the profile) ($\nu_1 = \nu_2$). (a) $B = 1.1$; (b) $B = 1.4$; (c) $B = 1.7$. Parameter-values are specified as follows: $\eta = 2$, $\varepsilon = 0.9$, $a = 0.1$, $\rho = 1\,\mathrm{kg/m^3}$, $f = 10^{-4}\,s^{-1}$, $C_D = 0.0015$, $\lambda_j = 0$ ($j = 1, 2, 3$), $r^* = 50$ km, $h_0 = 1\,000$ m, $\bar{h} = 5\,000$ m and $p_n = 1\,010$ mb

the intensity of the cyclone. In fact, the intensification-rate is very closely proportional to the square of the intensity, $(v^*)^2$, until an optimum intensity (at which $\{-\partial p_0/\partial t\ (r = 0)\}$ is greatest) is reached. In linear instability theory, on the other hand, the intensification rate $(\partial \varphi_j/\partial t)$ increases linearly with the intensity (by definition; see 4.1). In view of these results, it is not surprising that numerical tropical cyclone models have to be initialized with rather intense vortices, with an average maximum tangential wind speed of 12.2 m/s (Gray, 1978), before appreciable intensification occurs in a reasonable time in the integration.

The increasing efficiency of CISK as the cyclone intensifies will not continue forever, according to the present analysis. The reasons for the relatively abrupt arrest of the intensification at a certain intensity will be investigated further in the next section.

The exact shape of the tangential velocity profile does not appear to have a great influence on the results. When different H-profiles (with $B = 1.1$, 1.4, 1.7) are prescribed, the deepening stops when a certain minimum central surface pressure, p_c, is reached (see Fig. 12).

9. The Dependence of Cyclone-Intensification on the Size of the Eye Relative to the Local Rossby Radius

In Fig. 13 the surface pressure tendency is plotted against the mean radius of the eye divided by R_{loc} in the center of the cyclone for the "O-profile"

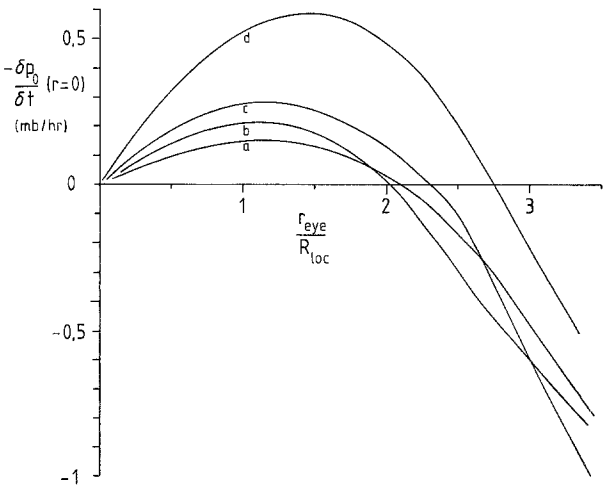

Fig. 13. The central surface pressure decrease-rate as a function of the mean radius of the eye (r_{eye}) divided by the local Rossby radius of deformation (R_{loc}) in the center of the cyclone, for vortices with an "O"-tangential velocity profile, for several combinations of $\bar{h}$, η and r^*. (a) $\bar{h} = 2\,000$ m, $r^* = 50$ km, $\eta = 2$; (b) $\bar{h} = 5\,000$ m, $r^* = 100$ km, $\eta = 2$; (c) $\bar{h} = 5\,000$ m, $r^* = 50$ km, $\eta = 2$; (d) $\bar{h} = 5\,000$ m, $r^* = 50$ km, $\eta = 2.5$. The value of other parameters are given in Fig. 6 ($\nu_1 = \nu_2$)

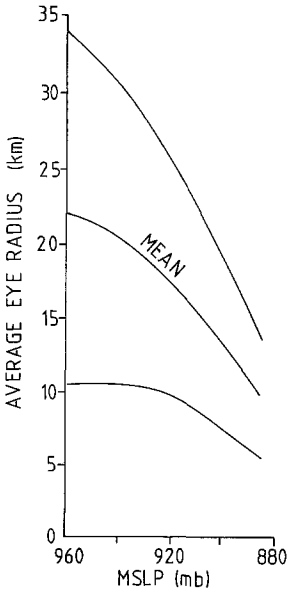

Fig. 14. Observed average (over 243 typhoons) eye-size (with standard deviation) for a given minimum sea-level pressure (MSLP) (adapted from Weatherford and Gray, 1988)

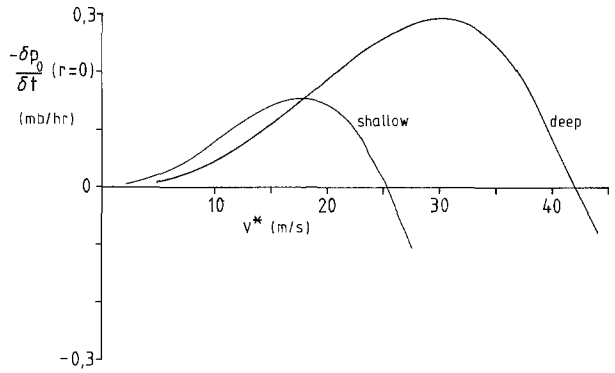

Fig. 15. The central surface pressure decrease-rate as a function of v^* (vortex-intensity) for a vortex with an "O"-tangential velocity profile with $r^* = 50$ km, for a shallow cyclone (total cyclone-depth: 5 000 m ($\bar{h} = 2\,000$ m)) and a deep cyclone (total cyclone-depth: 11 000 m ($\bar{h} = 5\,000$ m)). In both cases $\eta = 2$. The values of the other parameters are given in Fig. 6 ($v_1 = v_2$)

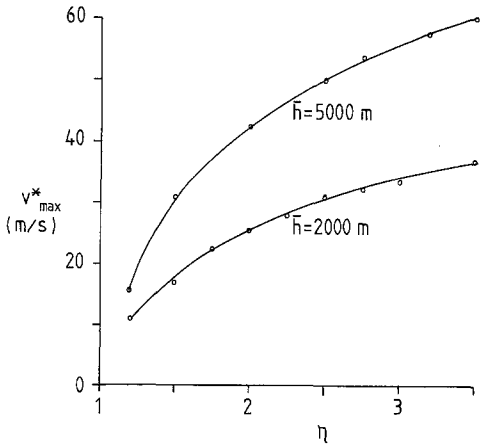

Fig. 16. The maximum attainable barotropic vortex-intensity, v^*_{max}, as a function of η for vortices with an "O"-tangential velocity profile and $\bar{h} = 5\,000$ m (representative of a tropical cyclone) and $\bar{h} = 2\,000$ m (representative of a polar low) ($r^* = 50$ km). The values of the other parameters are given in Fig. 6 ($v_1 = v_2$)

(we use this profile because R_{loc} is relatively constant inside the eye, making the physical interpretation of the problem easier) for several sets of parameter-values. *We see that further deepening of the cyclone is strongly inhibited if the radius of the eye is much larger than R_{loc}, i.e. if the heating is located "dynamically" too far away from the center of the cyclone.*

Observations in typhoons show that a contracting eye size is usually associated with central deepening, whereas an expanding eye size is usually associated with central filling (Weatherford and Gray, 1988). Also, extreme typhoons possess smaller eyes than minimal (less intense) typhoons. Fig. 14 shows the observed average eye-radius of typhoons as a function of central surface pressure. Especially noteworthy is that half of the weak typhoons with eyes have an eye with a radius of more than 30 km, whereas very few intense typhoons have an eye with a radius which is greater than 15 km. In view of the results displayed in Fig. 13, this now appears to be a dynamical necessity for the cyclone to subsist. Extreme typhoons can only remain extreme if they possess an eye with a radius of the same order of magnitude as R_{loc} in the core. Because R_{loc} inside an extreme typhoon is relatively small, the radius of the eye (R_{eye}) must also be relatively small. This may also explain the observed filling of hurricanes and typhoons when the inner eye-wall is replaced by an outer concentric eye-wall (Willoughby et al., 1982). The outer eye-wall convection is located too far away from the center of the cyclone to contribute to further central deepening. Of course, the present diagnostic model cannot explain why the original eye-wall is replaced by a new eye-wall further from the center, but it does offer a plausible answer to the question why this is accompanied by a decrease in the intensity.

Because R_{loc} decreases with decreasing depth, *a shallow cyclone will stop deepening earlier (at*

lower v) than a deep cyclone.* This is illustrated in Fig. 15 and 16. In Fig. 15 it can be seen that the deepening-rate of a shallow cyclone (such as a polar low) may be larger than the deepening rate of a deep cyclone (such as a tropical cyclone) with identical maximum tangential wind. But the decay-stage sets in earlier (at lower values of v^*) when the cyclone is shallow. Therefore, a polar low, with a typical depth of 5 km will never attain the same intensity through diabatic heating as a tropical cyclone, even if η is identical (see Fig. 16).

10. The Effect of Vortex-Baroclinicity

Until now barotropic ($v_1 = v_2$) vortices have been investigated. Obviously, this is not the whole story. Usually, the tangential wind velocity in hurricanes and polar lows *decreases* with height. This is a characteristic of any balanced warm-core cyclone. As far as can be judged from the results presented in his paper, Ooyama's (1969) model-simulations yielded $0.6\, v_1 < v_2 < v_1$. Therefore, it is appropriate to describe and discuss some calculations of the central deepening-rate for vortices with $v_2 < v_1$.

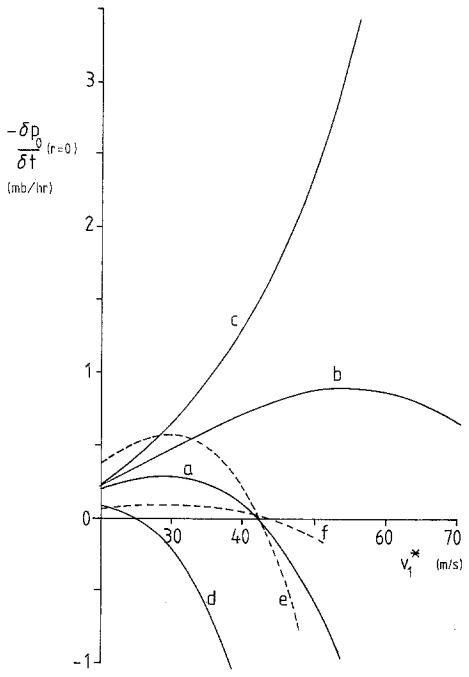

Fig. 17. The central surface pressure-tendency as a function of vortex-intensity (v_1*) ("O-profile"). The parameter-values in all cases are identical to those in Fig. 6, except (a) $v_2 = v_1$, $C_D = 0.0015$; (b) $v_2 = 0.8\, v_1$, $C_D = 0.0015$; (c) $v_2 = 0.6\, v_1$, $C_D = 0.0015$; (d) $v_2 = 1.5\, v_1$, $C_D = 0.0015$; (e) $v_2 = v_1$, $C_D = 0.003$; (f) $v_2 = v_1$, $C_D = 0.0005$

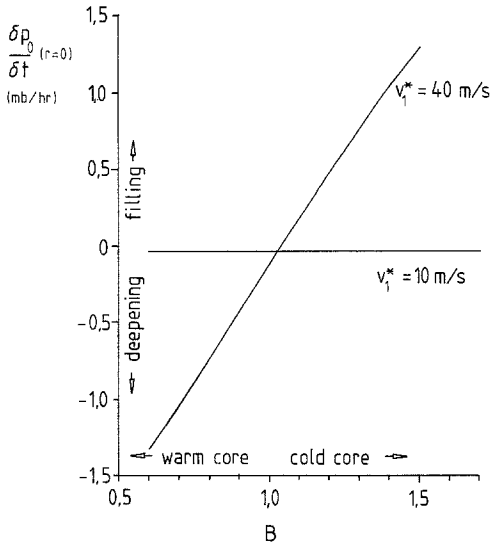

Fig. 18. The central surface pressure-tendency as a function of vortex-baroclinicity, B ($v_2 = Bv_1$), for two values of v_1* ("O-profile"). The other parameter-values are exactly as in Fig. 6

Fig. 17 shows a plot of the central surface pressure tendency as a function of the vortex-intensity, v_1*, for a vortex with an "O-profile" ($r^* = 50$ km), for three cases in which v_2 was a certain fixed fraction of v_1. It appears that *baroclinicity has very little effect on the deepening rate when the vortex is weak* ($v_1^* < 20$ m/s). However, when $v_1^* > 30$ m/s, the baroclinicity enhances the deepening-rate significantly. The central pressure-tendency may even fall below -3 mb/hr when $v_2 = 0.6\, v_1$ and $v_1^* > 55$ m/s. In this case there is no sign of an arrest of the intensification at high (but realistic) vortex- intensities. At $v_1^* \geqslant 60$ m/s no solution to (3.10) can be found, presumably because of symmetric baroclinic instability, which makes the balance-assumptions (3.2) and (3.3) invalid.

The increase of the deepening rates when $v_2 < v_1$ is due to the decrease of the inertial stability in layer 2. The resistance to radial displacements in this layer decreases and the outflow intensifies, while conditions in the inflow-layer remain more or less the same as in the barotropic case. This implies that a cold-core cyclone ($v_2 > v_1$) will generally not deepen by diabatic heating. This conjecture is confirmed by the calculation with $v_2 = 1.5\, v_1$ (curve *d* in Fig. 17).

For completeness, Fig. 17 also shows the sensitivity of the results to the choice of the drag coefficient. The computations for case (a) in Fig. 17 have been repeated for $C_D = 0.0005$ and $C_D = 0.003$ (the dashed lines). Apparently, the choice of C_D has no effect on the qualitative dependence of the deepening-rate on v_1* and, thus, also on the ratio R_{eye}/R_{loc}.

The dependence of the central deepening-rate on the baroclinicity of the cyclone is shown in Fig. 18 from another point of view. Clearly, a warm core is accompanied by enhanced deepening rates. Again, we see that a weak vortex (v_1* = 10 m/s or less) is hardly influenced by diabatic heating. A cold-core vortex will most probably fill under the influence of diabatic heating. All this implies that a cyclone, which may grow initially due to baroclinic instability or lee-cyclogenesis, will somehow have to acquire a warm core before diabatic heating can contribute significantly to further intensification.

11. Conclusion

In this paper we have discussed the effect of diabatic heating and boundary layer convergence on the deepening and filling of balanced cyclones. We have assumed that the heating is proportional to boundary layer convergence, which is determined by surface friction or drag, not eddy diffusion. *The results show that diabatic heating has very little effect on the surface pressure tendency when the cyclone is weak* (relative vorticity ~ planetary vorticity or less). On the other hand, *a relatively intense balanced warm-core cyclone may experience significant deepening due to diabatic heating*. But, the results also show that, *beyond a certain maximum cyclone-intensity, diabatic heating may induce a filling and expanding of the cyclone rather than a deepening*. This is expecially the case when the cyclone has a cold core, i.e. when the tangential velocity increases with height. Except by baroclinicity, the maximum intensity is also determined by the local Rossby radius of internal deformation in the core of the cyclone, which in turn is determined by the static stability in the troposhere, the depth of the cyclone and the vorticity of the tangential flow.

The depth of the cyclone is an important factor in determining the maximum attainable intensity. Inside relatively shallow cyclones the local Rossby radius of deformation, in the region where diabatic heating takes places (the eye-wall), becomes smaller than the eye-radius at lower vortex-intensities than in deep cyclones. This will inhibit further growth of a shallow cyclone in an earlier of its development.

The result that a relative weak cyclone is rather insensitive to diabatic heating, underlines the fact that *CISK must be interpreted as a finite-amplitude instability* accounting for the rapid or explosive intensification of a balanced cyclone by diabatic heating (which includes sensible heating and latent heat release).

Another (instability) mechanism must be responsible for the genesis of a balanced cyclone. The horizontal scale of the cyclone will probably be determined by this instability-mechanism. In the case of polar lows and other convectively dominated vortices at higher latitudes (e.g. the "bomb"; see Sanders and Gyakum, 1980), this could be baroclinic instability or lee-cyclogenesis (see e.g. Reed and Duncan, 1987, and Rasmussen, 1981). In the case of the tropical cyclone the mechanism behind the genesis-process is not so easily pin-pointed. Although several agents have been proposed, such as upper level baroclinic instability (Riehl, 1981) and easterly waves (Kurihara and Tuleya, 1984), one must also confront the difficult question of how a balanced flow regime can result from, for example, a random group of cumulus clouds. In other words, how can tropospheric heating produce a balanced flow? An example of this process in nature is the sea-breeze circulation. In its early stage, the sea-breeze blows from high to low pressure, but, because the heating over land continues for a period longer than $1/f$ (the timescale at which the earth's rotation becomes important), the flow adjusts to geostrophic balance. Therefore, at the end of the day, the sea-breeze blows along the coast. This process is illustrated in a numerical study by Neumann and Mahrer (1974) in the case of an island. By analogy, a balanced flow-regime can result over the tropical oceans only if diabatic heating (fixed relative to the mean flow) takes place on time scales comparable to, or larger than ($1/f$). Without the help of some other regulating mechanism, such as an easterly wave or baroclinic instability, this seems rather unlikely to happen, especially in the tropics, where f is small. But, once a sufficiently intense *balanced* flow has been established, it can take

control of the tropospheric heating through frictional convergence and/or by enhancing surface sensible heat fluxes due to the increased windspeeds, i.e. CISK can start to operate.

The results discussed above are based on a slightly modified version of Ooyama's (1969) model. The increased horizontal resolution in the center of the cyclone makes it possible to accurately calculate the central surface pressure tendency and capture the phenomenon of "cyclone-filling" at high cyclone-intensities. The vertical structure of the model is relatively coarse, especially in the boundary layer, and also the parametrization of diabatic heating is very unprezise. Moreover, the effect of pressure on the density is neglected. This effect is probably very important when there are large horizontal, as well as vertical pressure-gradients. Exact quantitative predictions can therefore not be expected from this model. Still, it is encouraging to see that, if some baroclinity is taken into account, the predicted deepening-rates are of the same order of magnitude as observed in real polar lows (Rasmussen, 1979), "bombs" (Gyakum, 1983) and tropical cyclones (Holliday and Thompson, 1979; Sheets, 1982; Weatherford and Gray, 1988). Also, the finding that the filling and deepening of a cyclone is related to the eye-size (relative to the internal Rossby radius in the core) is consistent with the findings of recent observational studies (see section 9).

Recently Emanuel (1986, 1987) has again stressed the important role of thermodynamics in tropical cyclones and polar lows. He proposes a new mechanism, called air-sea interaction instability (ASII), as an alternative to CISK. Emanuel points out that CISK requires conditional instability. By claiming that conditional instability is rare in the atmosphere, especially over the tropical oceans, he concludes that CISK is a "false hypothesis" (Emanuel, 1987). However, I would like to point out that conditional *in*stability is not needed in Ooyama's (1969) model to get cyclone-intensification. On the contrary, hydrostatic stability is imposed by definition (see section 3), thus excluding conditional instability explicitly. Subsequently a term (Eq. 3.6) is introduced which *only accounts for the vertical expansion of a hydrostatically balanced column of air due to a hypothetical heating. This may be any form of diabatic heating.* Because of the crude vertical representation, the distribution of this diabatic heat in the model-troposphere cannot be specified. In the model, "diabatic heating" functions as a disturbance to gradient wind balance. We have seen that the *stable* atmosphere reacts to this effect by readjusting to a *new* state of gradient wind balance, which in many cases, but not all, is such that the cyclone deepens. The exact expression for the effect of diabatic heating (e.g. Eq. 3.6) is, of course, very debatable. Eq. (3.6) demands an unlimited source of heat. But, it is not necessary to interpret this heating as latent heat release in cumulus clouds. The "CISK-mechanism" does not require conditional instability any more than for example a heat-low or a sea-breeze circulation require conditional instability. Why then, one may ask, does a heat low in summer not grow to hurricane-intensities? There are several reasons. In the first place, the heat-input is limited, and is distributed over a relatively large area. Secondly, a heat low is rather shallow and will thus never reach the stage of "explosive" development. Besides, even if this were the case, it is difficult to see how the balanced part of the flow could take control of this heating. In the case of the tropical cyclone, the sea represents a practically unlimited source of heat. This heat is pumped into the atmosphere in a *very small area* around the eye-wall, where the sensible heat fluxes are by far largest (due to the high wind-speeds) and latent heat release is most intense, probably due to enhanced frictional convergence. Therefore, although ASII is a valuable alternative way of interpreting the growth of cyclones through diabatic heating, I think it is unfair to discard CISK as a "false hypothesis".

Acknowledgements

I would like to thank Prof. Hans Vugts for giving me the time to continue this study at the Free University of Amsterdam.

Appendix A

Solution of the Equations for the Radial Circulation

Equations (2.7a, b) are solved by succesive relaxation on a grid, $x = 0, 1, 2 \ldots 89$, where

$$r = b(e^{\lambda x} - 1), \qquad \lambda = 0.1; \qquad b = 1\,000.$$

Therefore the first gridpoint ($x = 0$) corresponds to $r = 0$, the second gridpoint ($x = 1$) to $r = 105$ m and the last gridpoint ($x = 89$) to $r = 7\,331$ km. In between, the grid distance increases from about 200 m at $r = 1$ km ($x = 8$) to about 1 km at $r = 10$ km ($x = 25$), to about 10 km at $r = 98$ km ($x = 47$)

and about 20 km at $r = 200$ km ($x = 54$), etc. The high resolution in the center is needed to accurately calculate the surface pressure-tendency at $r = 0$ (see apendix B). At such small scales nonhydrostatic effects will be important. But, it appears reasonable to assume that *sustained surface* pressure changes, even at small scales, are not determined directly by non-hydrostatic effects.

The equations are transformed to the x-coordinate system $(\partial/\partial r = (dx/dr)(\partial/\partial x) = (1/(\lambda(r + b))(\partial/\partial x))$ and the x-derivatives are approximated by centered differences. The boundary conditions are $\psi_1 = \psi_2 = \psi_3 = 0$ at $x = 89$. The solution is considered acceptable if the change in ψ_1, ψ_2 and ψ_3 after one iteration step is less than 10^{-7} at all gridpoints. Convergence according to this *very strict criterium* (with an overrelaxation factor of 1.5) is attained after 400 to 550 steps starting from $\psi_1 = \psi_2 = \psi_3 = 0$ for all x.

Appendix B

Computation of the Central Surface Pressure-Tendency

The central surface pressure tendency is determined by the radial mass-flux out of the circular slab with radius r_1, where r_1 corresponds to the first gridpoint ($x = 1$ or $r_1 = 105$ m). The change in the mean thickness, **h**, of the slab is then given by

$$\frac{\mathrm{d}\mathbf{h}}{\mathrm{d}t} = \frac{2\pi r_1 h(r_1) u(r_1)}{\pi r_1^2}.$$

Therefore, the central surface pressure tendency is given by

$$\frac{\mathrm{d}p_0}{\mathrm{d}t} = g \sum_{j=1}^{3} \rho_j \frac{\mathrm{d}\mathbf{h}_j}{\mathrm{d}t} = \frac{2g}{r_1} \sum_{j=1}^{3} \rho_j h_j(r_1) u_j(r_1).$$

References

Billing, H., Haupt, I., Tonn, W., 1983: Evolution of a hurricane-like cyclone in the Mediterranean Sea. *Beitr. Phys. Atmos.*, **56**, 508.

Charney, J. G., Eliassen, A., 1964: On the growth of the hurricane depression. *J. Atmos. Sci.*, **21**, 68–75.

Delden, A. van., 1985: On the preferred mode of cumulus convection. *Beitr. Phys. Atmos.*, **58**, 202–219.

Eliassen, A., 1971: On the Ekman layer in a circular vortex. *J. Meteor. Soc. Japan*, **49**, 784–789.

Emanuel, K., 1986: An air-sea interaction theory for tropical cyclones. Part 1: Steady state maintanance. *J. Atmos. Sci.*, **43**, 585–604.

Emanuel, K., 1987: Large-scale and mesoscale circulations in convectively adjusted atmospheres. *Proceedings of the workshop on diabatic forcing*. ECMWF, Reading, UK, 323–348.

Frank, W. M., 1983: The cumulus parametrization problem. *Mon. Wea. Rev.*, **111**, 1859–1871.

Gray, W. M., 1978: Hurricanes: their formation, structure and likely role in the tropical circulation. In: *Meteorology over the Tropical Oceans*. 155–218. Royal Meteorological Society.

Gill, A. E., 1982: *Atmosphere-Ocean Dynamics*. New York, Academic Press. 662 pp.

Gyakum, J. R., 1983: On the evolution of the QE II storm. 1. Synoptic aspects. *Mon. Wea. Rev.*, **111**, 1137–1155.

Hack, J. J., Schubert, W. H., 1986: Nonlinear response of atmospheric vortices to heating by organized cumulus convection. *J. Atmos. Sci.*, **43**, 1559–1573.

Holland, G. J., 1980: An analytical model of the wind and pressure profiles in hurricanes. *Mon. Wea. Rev.*, **108**, 1212–1218.

Holland, G. J., Merrill, R. T., 1984: On the dynamics of tropical cyclone structural changes. *Quart. J. R. Met. Soc.*, **110**, 723–745.

Holliday, C. R., Thompson, A. H., 1979: Climatological characteristics of rapidly intensifying typhoons. *Mon. Wea. Rev.*, **107**, 1022–1034.

Kurihara, Y., Tuleya, R. E., 1981: A numerical simulation study on the genesis of a tropical cyclone. *Mon. Wea. Rev.*, **109**, 1629–1653.

Neuman, J, Mahrer, Y., 1974: A theoretical study of the sea and land breezes of circular islands. *J. Atmos. Sci.*, **31**, 2027–2039.

Ogura, Y., 1964: Frictionally controlled, thermally driven circulation in a circular vortex with application to tropical cyclones. *J. Atmos. Sci.*, **21**, 610–621.

Ooyama, K., 1964: A dynamical model for the study of tropical cyclone development. *Geofys. Intern.*, **4**, 187–198.

Ooyama, K., 1969: Numerical simulation of the life-cycle of tropical cyclones. *J. Atmos. Sci.*, **26**, 1–43.

Ooyama, K., 1971: A theory on the parameterization of cumulus convection. *J. Meteor. Soc. Japan*, **39**, 744–756.

Ooyama, K., 1982: Conceptual evolution of the theory and modelling of the tropical cyclone. *J. Meteor Soc. Japan*, **60**, 369–379.

Rasmussen, E., 1979: The polar low as an extratropical CISK-disturbance. *Quart. J. R. Meteor Soc.*, **16**, 313–326.

Rasmussen, E., 1981: An investigation of a polar low with a spiral cloud structure. *J. Atmos. Sci.*, **38**, 1785–1792.

Rasmussen, E, Lystad, M., 1987: The Norwegian polar lows project: a summary of the international conference on polar lows, 20–23 May 1986, Oslo, Norway, *Bull. Amer. Meteor. Soc.*, **68**, 801–816.

Rasmussen, E., Zick, C., 1987: A subsynoptic vortex over the Mediterranean with some resemblance to polar lows. *Tellus*, **39A**, 408–425.

Reed, R. J., Duncan, C. N., 1987: Baroclinic instability as a mechanism for serial development of polar lows: a case study. *Tellus*, **39A**, 376–384.

Riehl, H., 1981: Some aspects of the advance in the knowledge of hurricanes. *PAGEOPH*, **119**, 612–627.

Sanders, F., Gyakum, J. R., 1980: Synoptic-dynamic climatology of the "bomb". *Mon. Wea. Rev.*, **108**, 1589–1606.

Schubert, W. H., Hack, J. J., Silvas Dias, P. L., Fulton, S. R., 1980: Geostrophic adjustment in an axisymmetric vortex. *J. Atmos. Sci.*, **37**, 1464–1484.

Schubert, W. H., Hack, J. J., 1982: Inertial stability and tropical cyclone development. *J. Atmos. Sci.*, **39**, 1687–1697.

Schubert, W. H., DeMaria, M., 1985a: Axisymmetric, primitive equation, spectral tropical cyclone model. Part 1: Formulation. *J. Atmos. Sci.*, **42**, 1213–1224.

Schubert, W. H., DeMaria, M., 1985b: Axisymmetric, primitive equation, spectral tropical cyclone model. Part 2: normal mode initialization. *J. Atmos. Sci.*, **42**, 1225–1236.

Scorer, R. S., 1986: *Cloud Investigation by Satellite*. Ellis Horwood Series in environmental sciences.

Shapiro, L. J., Willoughby, H. E., 1982: The response of balanced hurricanes to local sources of heat and momentum. *J. Atmos. Sci.*, **39**, 378–394.

Sheets, R. C., 1982: On the structure of hurricanes as revealed by research aircraft data. In: *Intense Atmospheric Vortices* (ed. L. Bengtsson and J. Lighthill), 35–49.

Sundquist, H., 1970: Numerical simulation of the development of tropical cyclones with a ten-level model, Part 1. *Tellus*, **2**, 359–390.

Smith, R. K., 1981: The cyclostrophic adjustment of vortices with application to tropical cyclone modification. *J. Atmos. Sci.*, **38**, 2021–2030.

Weatherford, C. L., Gray, W. M., 1988: Typhoon structure as revealed by aircraft reconnaissance. Part 2: structural variability. *Mon. Wea. Rev.*, **116**, 1044–1056.

Willoughby, H. E., 1979: Forced secondary circulations in hurricanes. *J. Geoph. Res.*, **84**, 3173–3182.

Willoughby, H. E., Clos, J. A., Shoreibah, M. G., 1982: Concentric eye-walls, secondary wind maxima, and the evolution of the hurricane vortex. *J. Atmos. Sci.*, **39**, 395–411.

Yamasaki, M., 1977: The role of surface friction in tropical cyclones. *J. Meteor. Soc. Japan*, **55**, 559–571.

Author's address: Aarnout van Delden, University of Utrecht, Princetonplein 5, 3584 CC Utrecht, The Netherlands.